Braz J Phys (2017) 47:81–95
DOI 10.1007/s13538-016-0472-x

GENERAL AND APPLIED PHYSICS

Magnetohydrodynamic Shocks in the Interplanetary Space: a Theoretical Review

D. M. Oliveira[1,2]

Received: 27 September 2016 / Published online: 9 December 2016

Abstract I discuss in this brief review some properties of magnetohydrodynamic (MHD) discontinuities in the interplanetary space. My emphasis is on a special case of MHD discontinuity, namely interplanetary (IP) shocks, and those that are found at 1 AU. I derive the Rankine-Hugoniot (RH) equations to evaluate plasma parameters in the downstream region (shocked plasma) in relation to the upstream region (unshocked plasma). These properties are used to classify IP shocks in terms of their geometry and their direction of propagation in relation to the Sun. The shock geometry is determined in terms of two angles: θ_{B_n}, the angle between the upstream magnetic field and the shock normal, and θ_{x_n}, the angle between the shock normal and the Sun-Earth line. Sources of IP shocks frequently found in the solar wind at Earth's orbit are presented. Then the RH equations are solved for two categories of IP shocks in a special case: perpendicular shocks, when θ_{B_n} is 90°, and oblique shocks, when that angle is 45°. Finally, I highlight the importance of knowing the shock geometry, mainly the impact angle θ_{x_n}, specially whether the shock is frontal or inclined, for space weather-related investigations. IP shocks are known to be more geoeffective if they strike the Earth's magnetosphere frontally, or with impact angle nearly null. These results have been reported both by modeling and experimental studies in the literature.

✉ D. M. Oliveira
denny.m.deoliveira@nasa.gov

[1] NASA Goddard Space Flight Center, Greenbelt MD, USA

[2] Goddard Planetary Heliophysics Institute, University of Maryland Baltimore County, Baltimore, MD, USA

Keywords Space physics · Plasma physics · MHD discontinuities · Interplanetary shocks

1 Introduction

The interplanetary medium is surrounded by an electrically conducting fluid called plasma. When the moving plasma, or the solar wind, interacts with magnetic fields in its way, electric currents are induced, which in turn generate magnetic fields that change the plasma movement. The branch of science that describes the dynamics of the plasma motion is called magnetohydrodynamics, or simply MHD. The MHD theory corresponds to a coupled system of fluid equations and the Maxwell equations under special conditions. These equations are often employed in studies of plasma behavior. Plasmas have an interesting property related to the formation of discontinuities. Discontinuities are non-linear effects resulting from wave steepening. When MHD discontinuities are driven in this environment, conservation of mass, momentum, and energy are necessary to describe the plasma ahead and behind the discontinuity. These equations are called the Rankine-Hugoniot (RH) jump conditions. The type of discontinuity reviewed in this paper is a particular case of discontinuity called MHD shock that propagates in the interplanetary space, named interplanetary (IP) shocks. Other types of discontinuities are briefly mentioned in our review. In this case, references are given for the interested reader.

In this brief review, I derive the RH equations from basic MHD equations. RH equations are commonly used to study shock behavior, in particular the comparison between regions of unshocked and shocked plasmas. Conditions for the occurrence of discontinuities in the plasma are presented, in particular for the case of MHD shocks. I then

classify MHD shocks in terms of their shock normal angles in relation to the upstream magnetic field vector in the shock reference frame and their motion relative to the Sun. The main sources of MHD shocks in the interplanetary space, solar perturbations named coronal mass ejections (CMEs) and corotating interaction regions (CIRs), will be presented. Then I solve the RH equations for the particular cases of perpendicular and oblique shocks. Finally, we present some formulas generally used to calculate shock normal orientation and shock speed. These quantities have an important role in determining how IP shocks propagate in the interplanetary space. I then emphasize the importance of knowing the shock geometry in determining geomagnetic activity followed by the impact of IP shocks on the Earth's magnetosphere. This in turn is an important feature for the study of space weather-related phenomena.

2 Magnetohydrodynamic Equations

2.1 The Vlasov Equation

Plasma is a kind of a fluid which contains approximately the same amount of particles with positive and negative charges [29]. This condition implies that a plasma is an almost electrically neutral fluid. Each class of particles, such as He^{2+}, O^{+}, and e^{-}, is named species s. Statistical studies involving large amounts of particles require the use of a space defined in six dimensions called the phase space. The phase space is defined in terms of the position $\mathbf{r} = (x, y, z)$ and velocity $\mathbf{v} = (v_x, v_y, v_z)$ vectors. The density of this large number of particles is then written in terms of a distribution function $f_s(\mathbf{r}, \mathbf{v}, t)$ for each species as shown below:

$$dn_s = f(\mathbf{r}, \mathbf{v}, t) d^3r d^3v \tag{1}$$

The above equation is useful to define macroscopic parameters in terms of different moments of the velocity $\mathbf{v}$. The moment of order zero in $\mathbf{v}$ is obtained by integrating (1) over all the phase space, and the result is the particle number density for each species in the system:

$$n_s = \int_{-\infty}^{+\infty} f_s(\mathbf{r}, \mathbf{v}, t) d^3v \tag{2}$$

The first-order moment is obtained by integrating (1) again with the first power of $\mathbf{v}$. This is the average velocity distribution for each species in the system (the integral limits are dropped but the integral is still calculated over all the space phase):

$$\mathbf{v}_s = \frac{1}{n_s} \int \mathbf{v} f_s d^3v \tag{3}$$

The second moment of the distribution function is the pressure tensor [4]

$$\bar{P} = m_s \int (\mathbf{v} - \mathbf{v}_s)(\mathbf{v} - \mathbf{v}_s) f_s d^3v \tag{4}$$

Equations (1–4) define macroscopic parameters. Macroscopic MHD equations are derived from the distribution function f_s. Taking the time derivative of the distribution function, where $i = 1, 2, 3$ below, one gets

$$\begin{aligned} \frac{df_s}{dt} &= \frac{\partial f_s}{\partial t} + \sum_{i=1}^{3} \frac{\partial f_s}{\partial x_i} \frac{\partial x_i}{\partial t} + \sum_{i=1}^{3} \frac{\partial f_s}{\partial v_i} \frac{\partial v_i}{\partial t} \\ &= \frac{\partial f_s}{\partial t} + \mathbf{v} \cdot \nabla f_s + \mathbf{a} \cdot \nabla_v f_s \end{aligned}$$

The mean free path of particles in the interplanetary plasma is of the order of nearly 1 AU, or approximately 150 million km. Collisions in the interplanetary plasma occur approximately once every 10^8 s. Thus, this plasma is assumed to be collisionless. If the interplanetary plasma is collisionless, the time derivative of the distribution function vanishes [52]. As a result, the above equation, known as the Vlasov equation, can be written as

$$\frac{\partial f_s}{\partial t} + \mathbf{v} \cdot \nabla f_s + \mathbf{a} \cdot \nabla_v f_s = 0 \tag{5}$$

The forces acting on the interplanetary plasma are strictly electromagnetic forces. Gravitational and rotational forces may be neglected for our purposes [44]. From Newton's second law and the Lorentz force

$$m_s \mathbf{a} = q_s (\mathbf{E} + \mathbf{v} \times \mathbf{B}), \tag{6}$$

the Vlasov equation is given by

$$\frac{\partial f_s}{\partial t} + \mathbf{v} \cdot \nabla f_s + \frac{q_s}{m_s} (\mathbf{E} + \mathbf{v} \times \mathbf{B}) \cdot \nabla_v f_s = 0 \tag{7}$$

The electric and magnetic fields are obtained from the Maxwell equations. The Vlasov equation as represented above shall be used to determine the MHD one-fluid theory macroscopic equations.

2.2 The Maxwell Equations in the MHD Context

As mentioned above, a plasma is composed of positive and negative particles. Therefore, the plasma motion depends on the electric and magnetic fields $\mathbf{E}$ and $\mathbf{B}$ and is governed by Maxwell's equations as described below [23]:

$$\nabla \cdot \mathbf{E} = \frac{\rho_q}{\varepsilon_0} \tag{8}$$

$$\nabla \cdot \mathbf{B} = 0 \tag{9}$$

$$\nabla \times \mathbf{E} = -\frac{\partial \mathbf{B}}{\partial t} \tag{10}$$

$$\nabla \times \mathbf{B} = \mu_0 \mathbf{J} + \mu_0 \varepsilon_0 \frac{\partial \mathbf{E}}{\partial t} \tag{11}$$

These equations need some adjustments to be included in the MHD theory. The charge density ρ_q in the interplanetary plasma is null due to the plasma quasi-neutrality condition. The speed of light is defined as $c = 1/\sqrt{\mu_0\varepsilon_0}$. Considering the MHD characteristic dimensions for length, time, and speed as L, τ, and U (non-relativistic speed), the spatial and time derivative of $\mathbf{B}$ and $\mathbf{E}$ can be written as approximately $|\nabla \times \mathbf{B}| \approx B/L$ and $\mu_0\varepsilon_0|\partial\mathbf{E}/\partial t| \approx E/(c^2\tau)$ from the dimensional analysis of Faraday's law (10), one gets $E = UB$. Thus, by comparing the above derivatives,

$$\frac{\mu_0\varepsilon_0\partial\mathbf{E}/\partial t}{|\nabla \times \mathbf{B}|} \approx \frac{E/(c^2\tau)}{B/L} = \frac{U^2}{c^2} \ll 1 \tag{12}$$

Using these assumptions, the Maxwell equations in the MHD context are defined by

$$\nabla \cdot \mathbf{E} = 0 \tag{13}$$
$$\nabla \cdot \mathbf{B} = 0 \tag{14}$$
$$\nabla \times \mathbf{E} = -\frac{\partial \mathbf{B}}{\partial t} \tag{15}$$
$$\nabla \times \mathbf{B} = \mu_0 \mathbf{J} \tag{16}$$

By taking the divergent of Ampère's law (16), it is possible to show that $\nabla \cdot \mathbf{J} = 0$, which implies that currents are closed within plasmas. The current density is written in terms of the velocity $\mathbf{J} = ne\mathbf{v}$, which then implies that $\nabla \cdot \mathbf{v} = 0$.

2.3 The Adiabatic State Equation

In thermodynamics, a gas can expand rapidly enough without exchanging heat with the external medium. Such process is called an adiabatic process [45]. From the first law of thermodynamics, which is the energy conservation law for thermodynamic fluids, it is possible to show that the adiabatic fluid obeys the relation PV^γ = constant, where γ is the ratio of the heat capacity with constant pressure to the heat capacity with constant volume. This equation can be written in a conservative form as

$$\frac{d}{dt}\left(\frac{P}{\rho^\gamma}\right) = 0\,. \tag{17}$$

The adiabatic state equation will be useful later in deriving MHD macroscopic equations in conservative forms.

2.4 Multi-Fluid Theory: Macroscopic Equations

The problem analysis in plasma physics goes beyond the definition of the distribution function f_s. Often, it is necessary to write equations in terms of average macroscopic quantities calculated from the distribution function. Such average macroscopic quantities are described by the moment equations. The moment equations are calculated from the Vlasov equation by multiplying (7) by powers of the velocity $\mathbf{v}$.

The zeroth macroscopic equation or zeroth moment equation is obtained from the Vlasov equation by multiplying (7) by v^0 and integrating it in the velocity space V. Assuming a generic acceleration $\mathbf{a}$ instead of the Lorentz acceleration, this equation is written by

$$\int_V \frac{\partial f_s}{\partial t} d^3v + \int_V \mathbf{v} \cdot \nabla f_s d^3v + \int_V \mathbf{a} \cdot \nabla_v f_s d^3v = 0 \tag{18}$$

The first term of the above equation is the time derivative of the particle number density for each species s:

$$\int_V \frac{\partial f_s}{\partial t} d^3v = \frac{\partial n_s}{\partial t} \tag{19}$$

The second term can be rearranged as

$$\int_V \mathbf{v} \cdot \nabla f_s d^3v = \nabla \cdot \int_V \mathbf{v} f_s d^3v = \nabla \cdot (n_s \mathbf{v}_s) \tag{20}$$

The third term is rewritten using the Gauss theorem:

$$\int_V \nabla_v \cdot (\mathbf{a} f_s) d^3v = \int_S (\mathbf{a} f_s) \cdot d\mathbf{S} = 0 \tag{21}$$

This term vanishes because the distribution function f_s is null at infinity. As a result, by plugging (19–21) in (18), one gets

$$\frac{\partial n_s}{\partial t} + \nabla \cdot (n_s \mathbf{v}_s) = 0$$

Multiplying the above equation by m_s, where $\rho_s = m_s n_s$, one obtains the first macroscopic equation or the mass conservation equation for each species s:

$$\frac{\partial \rho_s}{\partial t} + \nabla \cdot (\rho_s \mathbf{v}_s) = 0 \tag{22}$$

The first moment equation is obtained by multiplying the Vlasov (7) by the first power in velocity $\mathbf{v}$ and integrating it all over the space velocity:

$$\int_V \mathbf{v} \frac{\partial f_s}{\partial t} d^3v + \int_V \mathbf{v}(\mathbf{v} \cdot \nabla f_s) d^3v + \int_V \mathbf{v}(\mathbf{a} \cdot \nabla_v f_s) d^3v = 0 \tag{23}$$

Using (3), the first term of the above equation can be written as:

$$\int_V \mathbf{v} \frac{\partial f_s}{\partial t} d^3v = \frac{\partial}{\partial t} \int_V \mathbf{v} f_s d^3v = \frac{\partial}{\partial t}(n_s \mathbf{v}_s) \tag{24}$$

Here, I use dyadics which result from the product between two vectors [34]. In dyadic algebra, assuming $\nabla \cdot \mathbf{v} = 0$, one can get the following identity:

$$\nabla \cdot (\mathbf{v}\mathbf{v} f) = \mathbf{v}(\mathbf{v} \cdot \nabla f) \tag{25}$$

Then after some manipulations with the term $\mathbf{vv}$ and using (2) and (3), the second term of (23) is given by

$$\int_V \mathbf{v}(\mathbf{v}\cdot\nabla f_s)d^3v = \nabla\cdot\int_V \mathbf{vv} f_s d^3v$$
$$= \nabla\cdot\int_V (\mathbf{v}-\mathbf{v}_s)(\mathbf{v}-\mathbf{v}_s) f_s d^3v + \int_V [\mathbf{v}_s\mathbf{v} + \mathbf{v}\mathbf{v}_s - \mathbf{v}_s\mathbf{v}_s] f_s d^3v$$
$$= \nabla\cdot\left[\int_V (\mathbf{v}-\mathbf{v}_s)(\mathbf{v}-\mathbf{v}_s) f_s d^3v + (n_s\mathbf{v}_s\mathbf{v}_s)\right]$$

Using (4), the second integral in (23) is

$$\int_V \mathbf{v}(\mathbf{v}\cdot\nabla f_s)d^3v = \frac{1}{m_s}\nabla\cdot\bar{P}_s + \nabla\cdot(n_s\mathbf{v}_s\mathbf{v}_s) \tag{26}$$

Now, we integrate the third term of (23) by parts. Assuming the distribution function vanishes at infinity, the last term in (23) can be written as

$$\int_V \mathbf{v}(\mathbf{a}\cdot\nabla_v f_s)d^3v = -\mathbf{a}\int_V f_s d^3v = -\mathbf{a}n_s \tag{27}$$

In the case of a plasma, the above acceleration is the Lorentz acceleration given by (6). The total charge is given by $q_s = n_s e_s$, where e_s is the electric charge of each species. The Lorentz acceleration is then $\mathbf{a} = n_s e_s[\mathbf{E} + \mathbf{v}_s \times \mathbf{B}]/m_s$. Thus, by grouping all terms obtained from (23), we get

$$\frac{\partial}{\partial t}(n_s\mathbf{v}_s) + \frac{1}{m_s}\nabla\cdot\bar{P}_s + \nabla\cdot(n_s\mathbf{v}_s\mathbf{v}_s) - \frac{n_s e_s}{m_s}[\mathbf{E}+\mathbf{v}_s\times\mathbf{B}] = 0 \tag{28}$$

Therefore, by multiplying the above equation by m_s with some simplifications, one gets the first moment equation or the MHD momentum equation:

$$\rho_s\left[\frac{\partial\mathbf{v}_s}{\partial t} + (\mathbf{v}_s\cdot\nabla)\mathbf{v}_s\right] + \nabla\cdot\bar{P}_s - n_s e_s[\mathbf{E}+\mathbf{v}_s\times\mathbf{B}] = 0 \tag{29}$$

The operator $\partial/\partial t + \mathbf{v}\cdot\nabla$ is named the convective derivative.

2.5 MHD One-Fluid Theory

In the last section, we presented the macroscopic equations for different plasma species s. In the interplanetary plasma, such species are mostly protons, and only 5 % are either heavier atoms or molecules. Without loss of generality, it is possible to approach the interplanetary plasma composition to approximate equal portions of protons and electrons. The MHD one-fluid theory consists then in combining the conservation equations of mass and momentum for protons and electrons.

In order to write these equation in terms of only one fluid, we assume that the mass of protons are much larger than the mass of electrons, or $m_p \gg m_e$. Therefore, the dominant species in the plasma is the proton species, and all quantities with index s may be written in terms of proton quantities. In resistive MHD, pressure is assumed to be a scalar [20]. As a result, without loss of generality, we can drop the proton index and rewrite the mass and momentum equations in conservative forms given by

$$\frac{\partial}{\partial t}(\rho\mathbf{v}) + \nabla\cdot(\rho\mathbf{v}) = 0 \tag{30}$$

$$\rho\left[\frac{\partial\mathbf{v}}{\partial t} + (\mathbf{v}\cdot\nabla)\mathbf{v}\right] + \nabla P - \rho_q\mathbf{E} - \mathbf{J}\times\mathbf{B} = 0 \tag{31}$$

The term dependent on $\mathbf{J}$ in the momentum equation can be substituted by the Ampère law (16) to give $\mathbf{J}\times\mathbf{B} = (\nabla\times\mathbf{B})\times\mathbf{B}/\mu_0$. Due to the fact that plasmas are electrically neutral, the electric charge density ρ_q vanishes. Thus, the momentum equation can be written as

$$\frac{\partial}{\partial t}(\rho\mathbf{v}) + \nabla\cdot(\rho\mathbf{v}\mathbf{v}) + \nabla P - \frac{1}{\mu_0}(\nabla\times\mathbf{B})\times\mathbf{B} = 0 \tag{32}$$

We now seek for one more equation to complete our set of MHD conservative equations. This equation is the second moment equation or the energy equation. As the plasma is electrically neutral, the charge density is zero. This task can be accomplished by multiplying (32) by $\mathbf{v}$:

$$\rho\mathbf{v}\cdot\left[\frac{\partial\mathbf{v}}{\partial t} + (\mathbf{v}\cdot\nabla)\mathbf{v}\right] + (\mathbf{v}\cdot\nabla)P - \frac{\mathbf{v}}{\mu_0}\cdot[(\nabla\times\mathbf{B})\times\mathbf{B}] = 0 \tag{33}$$

The first term in (33) obeys the following identity:

$$\rho\mathbf{v}\cdot\left[\frac{\partial\mathbf{v}}{\partial t} + (\mathbf{v}\cdot\nabla)\mathbf{v}\right] = \frac{\partial}{\partial t}\left(\frac{1}{2}\rho v^2\right) + \nabla\cdot\left(\frac{1}{2}\rho v^2\mathbf{v}\right) \tag{34}$$

Now let us use the adiabatic state (17). Using the convective derivative, expanding the time derivative on the right-hand side, and using the mass conservation (30), one gets

$$\frac{\partial P}{\partial t} + (\mathbf{v}\cdot\nabla)P = \frac{\gamma P}{\rho}\left[\frac{\partial\rho}{\partial t} + (\mathbf{v}\cdot\nabla)\rho\right]$$
$$= -\gamma P\nabla\cdot\mathbf{v} \tag{35}$$

Using the identity $P(\nabla\cdot\mathbf{v}) = \nabla\cdot(P\mathbf{v}) - \mathbf{v}\cdot\nabla P$ and solving for the second term in (35), we get

$$(\mathbf{v}\cdot\nabla)P = \frac{1}{\gamma-1}\frac{\partial P}{\partial t} + \frac{\gamma}{\gamma-1}\nabla\cdot(P\mathbf{v}) \tag{36}$$

The last term in (33) is given by

$$\mathbf{v}\cdot(\nabla\times\mathbf{B})\times\mathbf{B} = -\frac{\partial}{\partial t}\left(\frac{1}{2}B^2\right) - \nabla\cdot(\mathbf{E}\times\mathbf{B}) \tag{37}$$

Finally, after collecting all terms, the macroscopic MHD energy equation can be written as

$$\frac{\partial}{\partial t}\left(\frac{1}{2}\rho v^2 + \frac{P}{\gamma-1} + \frac{B^2}{2\mu_0}\right) +$$
$$\nabla\cdot\left[\frac{1}{2}\rho v^2\mathbf{v} + \frac{\gamma P}{\gamma-1}\mathbf{v} + \frac{1}{\mu_0}(\mathbf{E}\times\mathbf{B})\right] = 0 \tag{38}$$

In these equations, ρ is the plasma density, $\mathbf{B}$ is the magnetic field, $\mathbf{v}$ is the plasma bulk speed, $P/(\gamma - 1)$ is the internal energy, and $\gamma P/(\gamma - 1)$ is the enthalpy of the system. In summary, the conserved quantities are described as follows. Equation (30) indicates conservation of mass along the discontinuity. The other two equations indicate conservation of both momentum (31) and energy (38), respectively.

As described in the literature [44], a plasma can be studied in terms of its typical speeds, magnetic field, and some dimensionless parameters. In summary, such speeds are the sound speed

$$c_{\mathrm{S}} = \left(\frac{\gamma P}{\rho}\right)^{1/2}, \tag{39}$$

the Alfvén speed

$$v_{\mathrm{A}} = \frac{B}{\sqrt{\mu_0 \rho}}, \tag{40}$$

and the magnetosonic speed,

$$v_{\mathrm{MS}} = \sqrt{\frac{1}{2}(v_A^2 + c_S^2) \pm \sqrt{(v_A^2 + c_S^2)^2 - 4c_S^2 v_A^2 \cos^2\theta_{B_n}}} \tag{41}$$

whose positive root indicates the fast magnetosonic speed, and the negative root indicates the slow magnetosonic speed.

The dimensionless plasma parameters are represented by the plasma beta, which is the ratio between the plasma pressure and the magnetic pressure:

$$\beta = \frac{2\mu_0 P}{B^2}, \tag{42}$$

and other parameters called Mach numbers, the ratio of the fluid speed v' to the characteristic medium speed. Such Mach numbers are the sonic Mach number:

$$M_{\mathrm{S}} = \frac{v'}{c_S}, \tag{43}$$

the Alfénic Mach number

$$M_{\mathrm{A}} = \frac{v'}{v_A}, \tag{44}$$

and, in the same sense, the magnetosonic Mach number is written as

$$M_{\mathrm{MS}} = \frac{v'}{v_{MS}}. \tag{45}$$

In the particular case of MHD shocks, the speed considered is the speed of the shock in a frame of reference moving with the shock. If v_s is the shock speed along the shock normal, one changes $v' \to |v_s - v_p|$ in the expressions (43–45), where v_p is the plasma speed in the Earth's frame of reference.

3 Magnetohydrodynamic Shocks

3.1 The RH Equations for MHD Discontinuities

A shock is formed in a medium when a wave suffers a discontinuity in which its main parameters change, such as the fluid density, temperature (pressure), and velocity [7, 9, 49]. A necessary condition is that the relative speed between the shock and the fluid flow has to be greater than the sound speed in the non-shocked side of the discontinuity. Also, with the increase of pressure and temperature, one can affirm that the entropy increases beyond the shock, which indicates that the kinetic energy of the wave gives rise to the increase in thermal energy of the shocked fluid. Such descriptions are valid for a regular fluid, where particles change energy and momentum due to collisions. In the case of the solar wind, average densities are typically 5 particles per cm^3 at 1 AU. With mean free path of the order of the dimensions of the medium, which is approximately 1 AU, calculated from kinetic theory, collisions in the plasma are unlikely to occur [52]. Instead, momentum and energy are transmitted among particles due to the presence of the magnetic field, which makes the process even more complicated. Now, not only the magnetic field magnitude matters but also its direction in relation to the shock normal is important [9]. The presence of the magnetic field also adds two other complications: First, the plasma does not have only a typical speed such as the sound speed, since the concepts of Alfvén speed and the fast magnetosonic speed are necessary to explain the wave behavior of the plasma. Second, the shock geometry plays an important role in the shock physics since the magnetic field vector orientation in relation to the shock normal has different consequences when this angle is large or small. This last feature will be discussed further. As a result, a shock only exists when its relative speed between the shock and the medium is larger than the magnetosonic speed, or according to expression (45), when $M_{\mathrm{MS}} \geq 1$ [9].

The Rankine-Hugoniot (RH) jump conditions are derived from the MHD macroscopic equations written in conservative forms. These equations are (30), the mass conservation equation, (31), the momentum equation, and (38), the energy equation, written slightly different after some minor manipulations:

$$\frac{\partial}{\partial t}(\rho \mathbf{v}) + \nabla \cdot (\rho \mathbf{v}) = 0 \tag{46}$$

$$\frac{\partial}{\partial t}(\rho \mathbf{v}) + \nabla \cdot \left[\rho \mathbf{v}\mathbf{v} + \left(P + \frac{B^2}{2\mu_0}\right)\mathbf{1} - \frac{\mathbf{B}\mathbf{B}}{\mu_0}\right] = 0 \tag{47}$$

$$cm\frac{\partial}{\partial t}\left(\frac{1}{2}\rho v^2 + \frac{P}{\gamma - 1} + \frac{B^2}{2\mu_0}\right) + \nabla \cdot \left[\frac{1}{2}\rho v^2 \mathbf{v} + \frac{\gamma P}{\gamma - 1}\mathbf{v} + \frac{1}{\mu_0}(\mathbf{E} \times \mathbf{B})\right] = 0 \tag{48}$$

In order to relate plasma parameters in upstream (unshocked plasma) and downstream (shocked plasma) regions, let us consider a straightforward method as described in reference [20]. Figure 1 represents a plasma flowing through a very thin surface, with thickness $h \to 0$, across an MHD discontinuity of areas A_1 (unshocked side) and A_2 (shocked side) along, say, the normal $\mathbf{n}$, which is perpendicular to both surfaces. Integrating equation (46) and applying the Gauss theorem to its second term, we get:

$$\int_{V_1} \frac{\partial \rho_1}{\partial t} d^3x + \int_{V_2} \frac{\partial \rho_2}{\partial t} d^3x + \int_{V_2} \nabla \cdot (\rho \mathbf{v})_1 d^3x + \int_{V_1} \nabla \cdot (\rho \mathbf{v})_2 d^3x = 0$$
$$\int_{V_1} \frac{\partial \rho_1}{\partial t} d^3x + \int_{V_2} \frac{\partial \rho_2}{\partial t} d^3x + \int_{A_1} (\rho \mathbf{v})_1 \cdot d\mathbf{A}_1 + \int_{A_2} (\rho \mathbf{v})_2 \cdot d\mathbf{A}_2 = 0 \tag{49}$$

Now due to the very small box thickness, we can consider both volumes V_1 and V_2 shrinking to zero. This argument implies that the first two terms in (49) vanish. Assuming both surfaces are parallel to each other, $A_1 = A_2$. The scalar products in the two remaining parts of (49) are negative for A_1 and positive for A_2 due to the normal vector direction. We also define two unitary vectors, $\hat{\mathbf{n}}$, normal to the shock surface, and $\hat{\mathbf{t}}$, tangential to the normal surface. Therefore, (49) can be written in a conservative form as

$$\rho_1(\mathbf{v}_1 \cdot \mathbf{n}) = \rho_2(\mathbf{v}_2 \cdot \mathbf{n}) \tag{50}$$

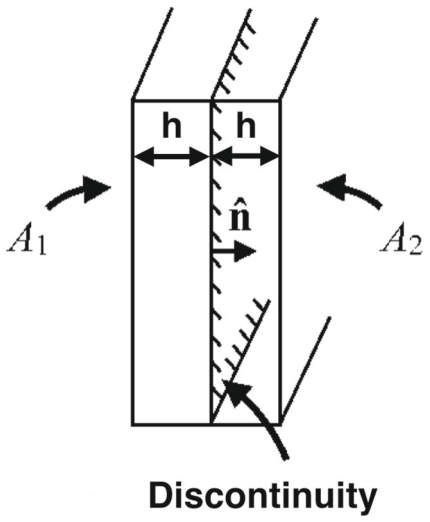

Fig. 1 Schematic representation of a tiny box across the surface of an MHD discontinuity. Assuming the box thickness to be infinitely small, or $h \to 0$, its volume shrinks to zero. Figure adapted from reference [20]

Applying the same method to the other (47–48), the RH jump conditions for conservation of mass. momentum, and energy are written as:

$$[\rho v_n] = 0 \tag{51}$$
$$\left[\rho v_n \mathbf{v} + \left(P + \frac{B^2}{2\mu_0}\right)\hat{\mathbf{n}} - \frac{B_n \mathbf{B}}{\mu_0}\right] = 0 \tag{52}$$
$$\left[\left(\frac{1}{2}\rho v^2 + \frac{\gamma P}{\gamma - 1}\right) v_n + \frac{1}{\mu_0}(\mathbf{E} \times \mathbf{B})_n\right] = 0 \tag{53}$$

The parameters of these equations are the same as those found in the MHD equations: $\mathbf{v}$ is the flow speed in the discontinuity reference frame, the indices n represent normal quantities, and the others are regular plasma parameters. Quantities between squared brackets, $[(\Psi)] = 0$, indicate that they are conserved along the discontinuity stream, i.e., $[\Psi] = \Psi_2 - \Psi_1$. Equation (51) represents the conservation of mass flux, (52) represents the conservation of momentum flux, and (53) represents the energy conservation.

These equations can still be written in a more straightforward way. The electric field in (53) can be eliminated by using $\mathbf{E} = -\mathbf{v} \times \mathbf{B}$ and the triple vector product identity $(\mathbf{F} \times \mathbf{G}) \times \mathbf{H} = (\mathbf{F} \cdot \mathbf{H})\mathbf{G} - (\mathbf{G} \cdot \mathbf{H})\mathbf{F}$. The scalar products of (52) with the unitary vectors $\hat{\mathbf{n}}$ and $\hat{\mathbf{t}}$ generate (55) and (56) below. The Maxwell equations require that the normal component of the magnetic field and the tangential component of the electric field are conserved through the discontinuity surface [23]. Then, the complete set of the RH jump conditions is given by

$$[\rho v_n] = 0 \tag{54}$$
$$\left[\rho v_n^2 + P + \frac{B_t^2}{2\mu_0}\right] = 0 \tag{55}$$
$$\left[\rho v_n v_t - \frac{B_n B_t}{\mu_0}\right] = 0 \tag{56}$$
$$\left[\left(\frac{1}{2}\rho v^2 + \frac{\gamma P}{\gamma - 1} + \frac{B^2}{\mu_0} - (\mathbf{v} \cdot \mathbf{B})\frac{B_n}{\mu_0}\right) v_n\right] = 0 \tag{57}$$
$$[B_n] = 0 \tag{58}$$
$$[E_t] = [\mathbf{v}_n \times \mathbf{B}_t + \mathbf{v}_t \times \mathbf{B}_n] = 0 \tag{59}$$

It should be mentioned at this point that MHD shock waves correspond to only one type of discontinuities found in the solar wind. Shock waves correspond to the most complicated type of MHD discontinuities due to the fact that all plasma parameters in the RH equations may vary. The other solar wind discontinuities are the contact discontinuity (CD), the tangential discontinuity (TD), and the rotational discontinuity (RD), first suggested by a theoretical work [30] Properties of different discontinuities in the solar wind have been discussed by several authors [14, 20, 22, 57, 64].

There is no plasma flow across a CD surface, which means $v_n = 0$. However, the plasma density suffers jumps across the CD surface, or $[\rho] \neq 0$. In the particular case of a CD in which $B_n = 0$, this discontinuity is called a TD. This difference was observed with Mariner 5 data [58]. In a TD, the plasma flow and magnetic field are parallel to the discontinuity surface. An RD has no jump in plasma density, $[\rho] = 0$, but plasma flows across an RD surface. Thermal pressure does not change across an RD surface, or $v_n \neq 0$. Table 1 summarizes the main properties of CDs, TDs, RDs, and shock waves. CDs are much more difficult to be identified due to the rapid diffusion of plasma along the surface magnetic field lines, and the jump becomes very smooth [8, 14]. However, more recently, the possibility of CD observations has been brought about [21]. Based on the rarity of identification and consequently the observation of solar wind discontinuities other than MHD shock waves, the former does not take part in the scope of this review. Therefore, from now on, we will only consider MHD shock waves propagating in the interplanetary space in our MHD discontinuity analyses.

3.2 Shock Normal Decomposition

To describe how IP shocks propagate in the interplanetary medium, it is necessary to define the shock normal in terms of polar angles θ_{x_n}, the angle between the shock normal and the Sun-Earth line, and clock angles φ_{y_n}, the angle between the shock normal with the Y axis. The ranges of these angles are $0 \leq \theta_{x_n} \leq \pi$ and $0 \leq \varphi_{y_n} \leq 2\pi$, respectively, as described elsewhere [37, 39, 65]. In spherical coordinates, the normal components of the vector $\mathbf{n} = (n_x, n_y, n_z)$ are given by the orthonormal system of coordinates

$$\begin{aligned} n_x &= \cos\theta_{x_n} \\ n_y &= \sin\theta_{x_n}\cos\varphi_{y_n} \\ n_z &= \sin\theta_{x_n}\sin\varphi_{y_n} \end{aligned} \tag{60}$$

which satisfy $|\mathbf{n}| = 1$ as a normalization condition. Therefore, translated from the shock frame of reference to a Cartesian frame of reference defined in GSE coordinates, the magnetic field (and also the speed) is written as

$$\begin{pmatrix} B_x \\ B_y \\ B_z \end{pmatrix} = \begin{pmatrix} \cos\theta_{x_n} & -\sin\theta_{x_n} & 0 \\ \sin\theta_{x_n}\cos\varphi_{y_n} & \cos\theta_{x_n}\cos\varphi_{y_n} & -\sin\varphi_{y_n} \\ \sin\theta_{x_n}\sin\varphi_{y_n} & \cos\theta_{x_n}\sin\varphi_{y_n} & \cos\varphi_{y_n} \end{pmatrix} \times \begin{pmatrix} B_n \\ B_t \\ 0 \end{pmatrix} \tag{61}$$

The RH equations are solved in the special frame of reference in which the shock is stationary. The magnetic field is invariant because the system is non-relativistic, so $\mathbf{B}' = \mathbf{B}$ where prime quantities are in the frame of reference where observations are made. All calculations are computed in the Hoffmann-Teller frame of reference, where $\mathbf{v} \parallel \mathbf{B}$ and as a result, the electric field vanishes in this reference frame [15]. Then it is necessary to calculate a Galilean transformation, from the shock frame of reference to another frame of reference that may be a spacecraft or the Earth. Therefore, defining the shock speed as $\mathbf{v}_s = v_s\mathbf{n}$, with $\mathbf{n}$ represented by (60), this transformed velocity is given by

$$\mathbf{v}' = \mathbf{v} + \mathbf{v}_s \tag{62}$$

3.3 Types of Shocks

The following discussion about types and classifications of shocks is based on descriptions found in the literature [9, 30], and in a more recent review [64]. As has already been discussed, the solar wind has different typical speeds. The magnetosonic speed depends both on the sound and the Alfvén speeds. When the relative shock speed, calculated in the shock frame of reference, is greater than the magnetosonic speed, the shock is classified as a fast shock. For the other case, the shock is said to be slow. If the shock propagates away from the Sun, it is classified as forward. Then, if the shock propagates toward the Sun, the shock is said to be reverse, although all shocks

Table 1 Classification of the MHD discontinuities accordingly to normal speed, normal magnetic field, and density variations across the discontinuity

	CD[a]	TD[b]	RD[c]	Shock wave
Normal speed	Null	Null	$\neq 0$	$\neq 0$
Jump in plasma density	$\neq 0$	$\neq 0$	Null	$\neq 0$
Normal magnetic field	Null	$\neq 0$	$\neq 0$	Null or $\neq 0$

[a]Contact discontinuity

[b]Tangential discontinuity. A TD is a particular case of a CD in which $B_n = 0$

[c]Rotational discontinuity

propagate toward the Earth because they are dragged by the solar wind [46]. As a result, shocks can be fast and slow forward, and fast and slow reverse. Figure 2 shows qualitatively how the plasma parameters vary after the shock takes place. In the case of IP shocks propagating in the interplanetary space, fast forward shocks (FFSs) are more frequent and cause more disturbances in the Earth's magnetosphere-ionosphere-thermosphere system [5, 16, 26, 39, 42, 56]. Plasma density, magnetic field, temperature, and speed have positive jumps in FFSs. In all cases, the shock speed is measured in the Earth's or spacecraft's frame of reference. Although less frequent than fast shocks, slow shocks have also been observed in the solar wind [10, 12, 68, 69].

Figure 3 represents a real FFS observed by the ACE satellite on 23 June 2000 at 1226 UT and (234,36.6,-0.7)R_E GSE upstream of the Earth. Typically, jumps in plasma parameters and magnetic field associated with FFS are very sharp, as can be seen in Fig. 3, from top to bottom: magnetic field, thermal plasma pressure, particle number density, speed, and dynamic pressure proportional to ρv^2. The increase in the dynamic pressure is a result of the shock compression and shock enveloping of the Earth's magnetosphere [11, 50, 59]. As a result, a myriad of events can be measured on the ground after the impact of an FFS [2, 71, 73].

The presence of the magnetic field vector in the space plasma introduces an additional complexity in relation to an ordinary gas because the angle between the magnetic field vector and the shock normal plays an important role inj determining downstream plasma parameters. Thus, an IP

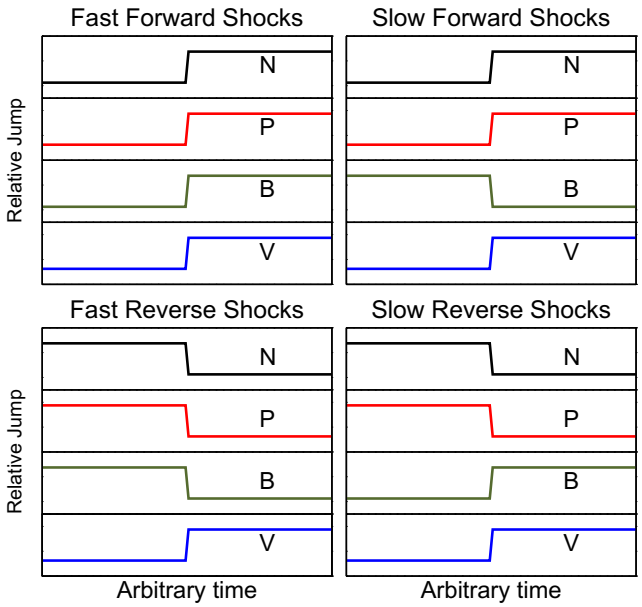

Fig. 2 Schematic variations of the parameters n, P, B, and v for the four types of interplanetary shocks. *Upper panels*: *left*, fast forward, and *right*, slow forward shocks. *Bottom panels*: *left*, fast reverse, and *right*, slow reverse shocks

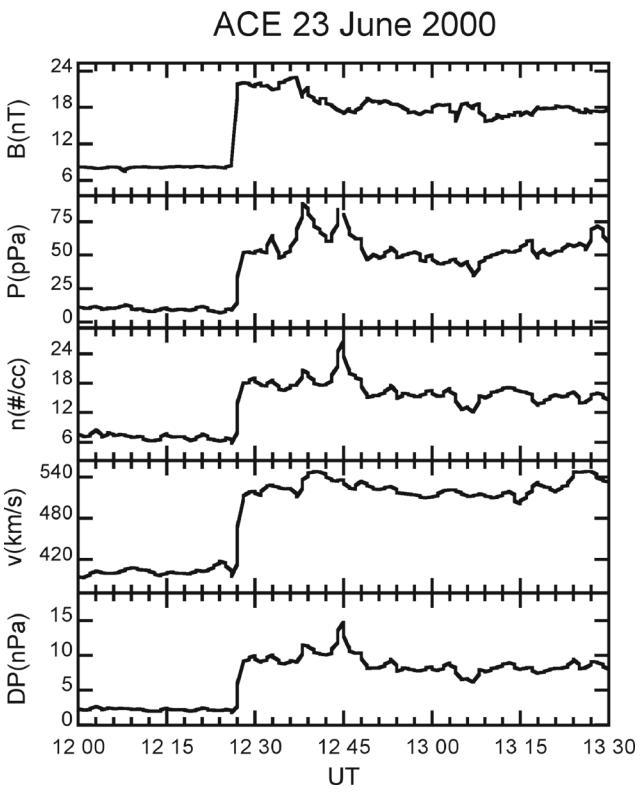

Fig. 3 An FFS observed by ACE spacecraft on 23 June 2000 at 1226 UT. Jumps in all plasma parameters are step-like and positive. The increase of the dynamic pressure ρv^2 indicates the occurrence of an IP shock as well

shock can be classified as either perpendicular or oblique [8, 9, 30]. A common choice is that for the former case, the angle between the magnetic field vector and the shock normal, the obliquity θ_{B_n}, is 90°. In the latter case, θ_{B_n} is 45°. When this angle is 0°, the shock is said to be parallel. Figure 4 shows both magnetic and velocity vectors in the shock frame of reference for an FFS case. On the top panel, the magnetic field lies in the plane perpendicular to the plane containing the shock normal. The downstream magnetic field increases and the velocity decreases. The same occurs in the case of an oblique shock, represented in the bottom panel of the same figure. Generally, the shock normal orientation is necessary to obtain θ_{B_n}, but it has been shown that it is possible to calculate the shock obliquity knowing only upstream and downstream plasma parameters [13].

The shock obliquity θ_{B_n} plays a significant role in energetic particle acceleration at interplanetary traveling shocks [31]. The critical shock Mach number (Mc) depends upon the upstream plasma β and the angle θ_{B_n} [17, 27]. If the shock has a Mach number greater than a determined Mc, the shock is said to be supercritical. If the shock is supercritical, electron resistivity and ion viscosity dissipations may occur at the shock. Recently, it has been shown that approximately

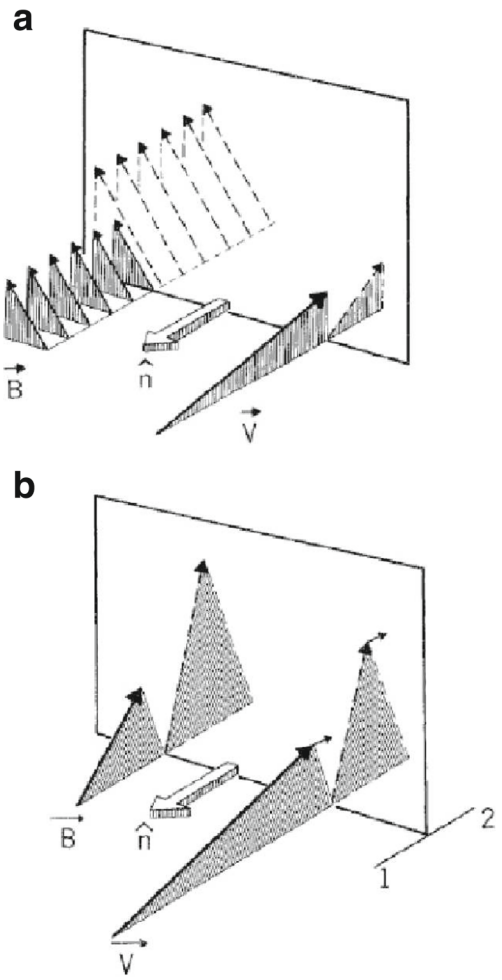

Fig. 4 Schematic representation of fast forward shocks (FFSs) in the shock reference frame. **a** represents a perpendicular shock in which the magnetic field vector lies in the plane perpendicular to the shock normal, the tangential plane. In this case, the magnitude of the magnetic field downstream increases in relation to its upstream magnitude. The opposite occurs to the velocity of the medium. **b** shows an oblique shock, with the magnetic field lying in both planes. The medium velocity increases in this case. The shock normal is defined pointing to the downstream, low entropy region. Figure adapted from the literature [9]

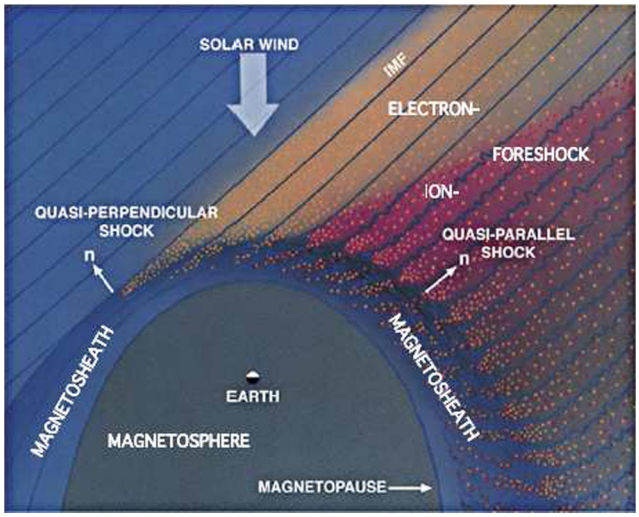

Fig. 5 Representation of the solar wind interaction with the Earth's bow shock [28]. Quasi-perpendicular and quasi-parallel shocks are shown. *Blue lines* represent the IMF. The shocked region is the magnetosheath

1/3 of IP shocks driven by CMEs are supercritical and 2/3 of IP shocks driven by CIRs are supercritical [72].

Now let us take the Earth's magnetosphere interaction with the solar wind. The first consequence of this interaction is the formation of a bow shock right in front of the Earth's magnetosphere [48]. Figure 5 shows that the bow shock is the diffuse hyperbolically shaped region standing at a distance in front of the magnetopause. The bow shock has a complicated magnetic structure, with a "foot", a "ramp", and an "overshoot". Overshoots occur in the bow shock due to the fact that jumps in magnetic field often exceed those predicted by the RH conditions [33, 35, 47]. The inclined blue lines represent the interplanetary magnetic field (IMF). In this figure, the IMF lies in the equatorial plane. The direction of the shock normal is indicated at two positions. Where it points perpendicularly to the IMF, the character of the bow shock is perpendicular. In the vicinity of this point where the IMF is tangent to the bow shock, the shock behaves quasi-perpendicularly. When the shock is aligned with or against the IMF, the bow shock behaves as a quasi-parallel shock. Quasi-perpendicular shocks are magnetically quiet compared to quasi-parallel shocks [3]. This is indicated here by the gradually increasing oscillatory behavior of the magnetic field when passing along the shock from the quasi-perpendicular part into the quasi-parallel part. Correspondingly, the behavior of the plasma downstream of the shock is strongly disturbed behind the quasi-perpendicular shock. The bow shock is often found to be supercritical.

Finally, when the shock is supercritical, as is the case for the bow shock, electrons and ions are reflected from it. Reflection is strongest at the quasi-perpendicular shock but particles can escape upstream only along the magnetic field. Hence, the upstream region is divided into an electron (yellow) and an ion foreshock accounting for the faster escape speeds of electrons than ions. More details on the shock behavior of the bow shock can be found in [48], and the interaction of solar wind discontinuities and interplanetary shocks are discussed by [70].

3.4 Sources of IP Shocks

The two major IP shock drivers are named coronal mass ejections (CMEs) [18] and corotating interaction regions (CIRs) [43]. CMEs are known to be well correlated with solar activity [25], but such relation is not obvious for

CIRs since their numbers do not vary noticeably throughout the solar cycle [24]. A schematic representation of an IP shock driven by a CME (or ICME, which is a CME propagating in the interplanetary medium) is shown in Fig. 6. CMEs are formed in the Sun's corona, the upper layer of the Sun's atmosphere. Although the corona could be seen during solar eclipses for centuries, CMEs were only observed after the space era with coronagraphs such as LASCO (Large Angle and Spectrometric Coronagraph Experiment) onboard the satellite SOHO (SOlar and Heliospheric Observatory). While propagating throughout the interplanetary space, solar wind discontinuities, or almost always IP shocks, are formed ahead of CMEs. Figure 7 shows an image taken by LASCO of a very strong CME that occurred on 18 November 2003. The shock/sheath region in the leading edge region is responsible for driving IP shocks. This region can be seen in Fig. 7.

An example of a CIR-related IP shock is schematically represented by Fig. 8 which shows that the rotating geometry of CIRs may propitiate a good condition for shock inclinations in relation to the Sun-Earth line. The view is from above the north pole of the Sun, looking down on the ecliptic plane. Spatial differences in the nearly radial expansion (indicated by the dark vectors) are coupled with solar rotation to produce compression regions (shaded) and rarefactions in the interplanetary medium. Secondary non-radial motions are driven by pressure gradients built up in the stream interaction (large open arrows). Magnetic field lines, which correspond to streamlines of flow in the rotating frame, are drawn out into the spiral configuration as shown in Fig. 8. Shocks may occur if the difference between the

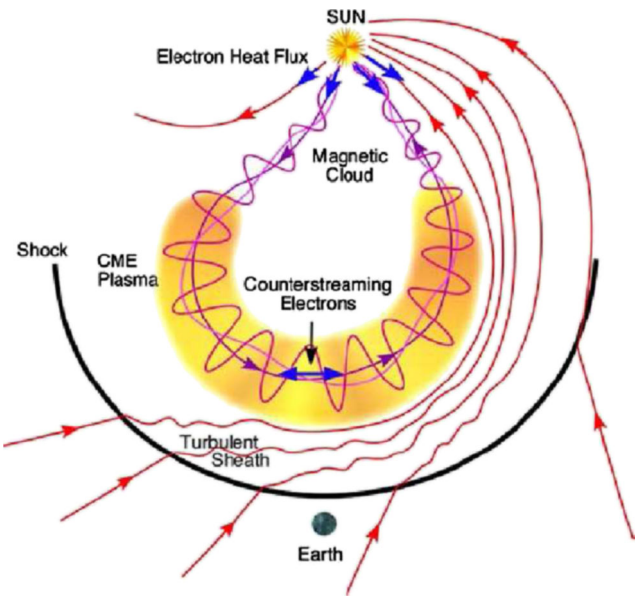

Fig. 6 Schematic representation of a shock formation in front of an ICME, as shown in [74]

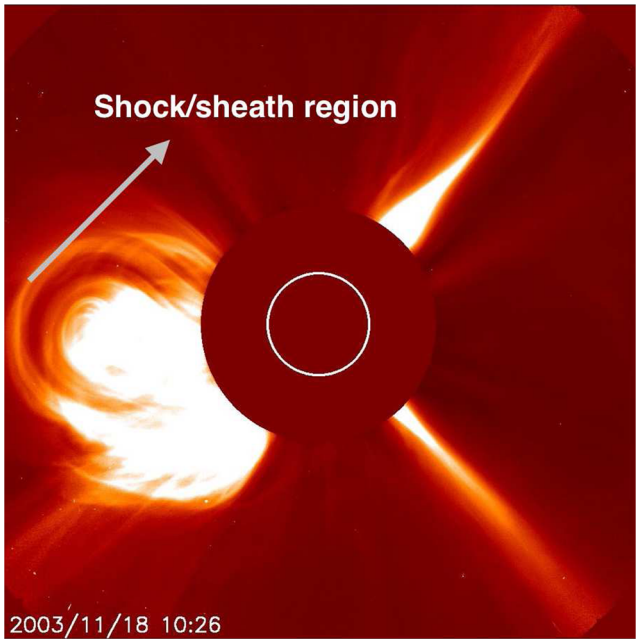

Fig. 7 A CME image taken by the LASCO telescope onboard the SOHO spacecraft on 18 November 2003 at 1026 UT. The CME shock/sheath region that drove an IP shock is seen in the image

fast speed stream and slow speed stream is greater than the magnetosonic speed of the medium. According to CIR evolution studies [60], most CIRs complete their evolution in the interplanetary space by 4.2 AU. Therefore, the number of CIR-driven shocks observed at 1 AU is relatively low.

IP shocks driven by these solar disturbances are different in several aspects, such as shock strength, radial propagation, and occurrence throughout the solar cycle [36]. As a result, geomagnetic activity followed by CMEs and CIRs may also lead to distinct observations, for example, intensity and duration of geomagnetic storms [6].

Often, IP shock structures are thought as planar structures that propagate in the interplanetary space [51]. Such structure allows the determination of a unitary vector perpendicular to the shock surface, usually pointing toward the Sun, named shock normal. IP shock normals driven by either CMEs or CIRs usually differ in orientation [24, 25]. CME-driven shocks tend to have their shock normals aligned with the Sun-Earth due to their mostly usual radial propagations, as shown by Fig. 6. On the other hand, shocks driven by CIRs are more likely to have their shock normal inclined in relation to the Sun-Earth line, as seen in Fig. 8. This happens due to the fact that fast and slow streams tend to follow the Parker spiral [43].

3.5 RH Solutions for MHD Shocks

In this section, we solve the RH equations for the specific cases of perpendicular and oblique shocks. Our task

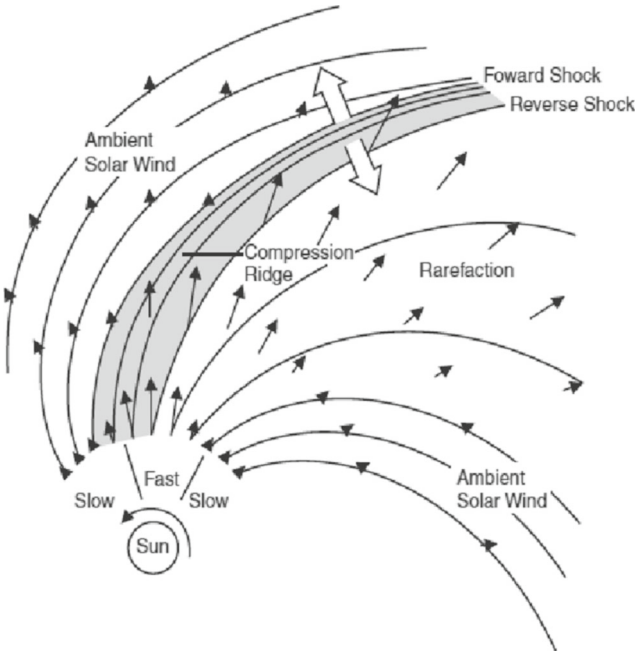

Fig. 8 Schematic representation of the stream interaction in the inertial frame after [43]. When the difference between the fast and slow streams becomes greater than the magnetosonic speed of the medium, a shock may occur

is to find relationships between upstream and downstream shock parameters. Equations (54–59) are written explicitly in terms of upstream (1) and downstream (2) parameters. The shock compression ratio is defined as the ratio of the downstream plasma density to the upstream plasma density, i.e., $X \equiv \rho_2/\rho_1$. From the mass conservation (54), this choice implies that $v_2/v_1 = X^{-1}$. All other conditions will depend on the compression ratio X.

In the case of perpendicular shocks, where $\theta_{B_n} = 90°$, the magnetic field lies in the plane which contains the discontinuity and does not have a normal component (see Fig. 4). Then, from the relation for the velocity, we get $B_2/B_1 = X$. By rewriting (55) explicitly with $v_n = v$ and $B_t = B$, we get

$$\rho_2 v_2^2 + P_2 + \frac{B_2^2}{2\mu_0} = \rho_1 v_1^2 + P_1 + \frac{B_1^2}{2\mu_0} \tag{63}$$

By dividing the above equation by P_1, using the sonic Mach number M_S (43), and (63), and the plasma beta (42), after some manipulations, we get

$$\frac{P_2}{P_1} = \gamma M_S^2 \left(1 - \frac{1}{X}\right) + \frac{1}{\beta}(1 - X^2) + 1 \tag{64}$$

Table 2 summarizes the results for the RH equations obtained in the case of perpendicular shocks.

The solutions for oblique shocks are more complicated because $\theta_{B_n} \neq 90°$ and all normal and tangential components of magnetic field and velocity are not null. Here, we choose the de Hoffmann-Teller reference frame, so $\mathbf{v}_1 \times \mathbf{B}_1 = \mathbf{v}_2 \times \mathbf{B}_2 = 0$. This choice yields the following relationships:

Table 2 RH solutions for perpendicular shocks

Perpendicular shocks, $\theta_{B_n} = 90°$	
Compression ratio	$X = \frac{\rho_2}{\rho_1}$
Velocity	$\frac{v_2}{v_1} = \frac{1}{X}$
Magnetic field	$\frac{B_2}{B_1} = X$
Plasma pressure	$\frac{P_2}{P_1} = \gamma M_S^2 \left(1 - \frac{1}{X}\right) + \frac{1}{\beta}(1 - X^2) + 1$

$$v_{1t} = \frac{v_{1n} B_{1t}}{B_{1n}} \quad \text{and} \quad v_{1t} = \frac{v_{2n} B_{2t}}{B_{2n}} \tag{65}$$

whose ratio is given by

$$\frac{v_{2t}}{v_{1t}} = \frac{1}{X}\frac{B_{2t}}{B_{1t}} \tag{66}$$

In order to find a relationship between the upstream and downstream velocity and magnetic field, we write (56) explicitly in terms of upstream and downstream parameters

$$\rho_2 v_{2n} v_{2t} - \frac{B_{2n} B_{2t}}{\mu_0} = \rho_1 v_{1n} v_{1t} - \frac{B_{1n} B_{1t}}{\mu_0} \tag{67}$$

and, after solving for v_{2t}/v_{1t} using the compression ratio and the Alfvèn speed, we get

$$\frac{v_{2t}}{v_{1t}} = \frac{v_1^2 - v_A^2}{v_1^2 - X v_A^2} \quad \text{and} \quad \frac{B_{2t}}{B_{1t}} = \frac{X(v_1^2 - v_A^2)}{v_1^2 - X v_A^2} \tag{68}$$

The choice of the de Hoffmann-Teller reference frame assures that all magnetic terms in (57) vanish. As a result, solving for P_2/P_1, we get

$$\frac{P_2}{P_1} = X + \frac{1}{2}(\gamma - 1) X M_S^2 v_1^2 \left(1 - \frac{v_2^2}{v_1^2}\right) \tag{69}$$

The results obtained for oblique shocks are summarized in Table 3.

Table 3 RH solutions for oblique shocks

Oblique shocks, $\theta_{B_n} \neq 90°$	
Compression ratio	$X = \frac{\rho_2}{\rho_1}$
Normal velocity	$\frac{v_{2n}}{v_{n1}} = \frac{1}{X}$
Tangential velocity	$\frac{v_{2t}}{v_{1t}} = \frac{v_1^2 - v_A^2}{v_1^2 - X v_A^2}$
Normal magnetic field	$\frac{B_{2n}}{B_{1n}} = X$
Tangential magnetic field	$\frac{B_{2t}}{B_{1t}} = \frac{X(v_1^2 - v_A^2)}{v_1^2 - X v_A^2}$
Plasma pressure	$\frac{P_2}{P_1} = X + \frac{1}{2}(\gamma - 1) X M_S^2 v_1^2 \left(1 - \frac{v_2^2}{v_1^2}\right)$

Figure 9 represents the solutions of (64) and (69), the ratio of downstream to upstream plasma thermal pressures, for perpendicular (upper panel) and oblique (lower panel) shocks, respectively. Here, P_2/P_1 are plotted as a function of the fast magnetosonic Mach number Ms. These ratios are plotted for different shock strengths, i.e., shocks with different compression ratios. The plasma compression in the shocked region is larger for stronger shocks. However, as one would expect, the plasma compression is higher in the cases of perpendicular shocks due to the shock symmetry. In general, impacts of almost perpendicular shocks trigger higher geomagnetic activity in comparison to oblique shocks under the same plasma and IMF conditions. This has already been reported in the literature with simulations and observations as well [26, 37–39, 41, 53, 54, 67].

3.6 Shock Speed and Normal Calculation Methods

Once one has the observed shock parameters, i.e., upstream and downstream plasma and IMF parameters, the shock speed can be calculated using the RH (54–59). Taking (54), it is possible to write the shock speed as

$$v_s = \frac{[\rho \mathbf{v}]}{[\rho]} \cdot \mathbf{n}\,, \tag{70}$$

where $\mathbf{v}$ is the relative speed of the shock in relation to the medium. However, the shock normal is still to be determined.

The IP shock normal is one of the most important features to be understood in a shock. Throughout the years, many single spacecraft shock normal methods have been suggested, such as the magnetic coplanarity [14, 32], velocity coplanarity and plasma/IMF data mixed methods [1], and the interactive scheme by [65], later improved by [62]. A summary of IP shock normal calculation methods can be found in [55].

Thus, the equations for the most important single spacecraft methods to determine shock normal orientations are the magnetic coplanarity,

$$\mathbf{n}_{MC} = \frac{\mathbf{B}_2 \times \mathbf{B_1} \times [\mathbf{B}]}{|\mathbf{B}_2 \times \mathbf{B_1} \times [\mathbf{B}]|}\,, \tag{71}$$

the plasma/IMF data mixed methods,

$$\mathbf{n}_{MX1} = \frac{(\mathbf{B}_1 \times [\mathbf{v}]) \times [\mathbf{B}]}{|(\mathbf{B}_1 \times [\mathbf{v}]) \times [\mathbf{B}]|} \tag{72}$$

$$\mathbf{n}_{MX2} = \frac{(\mathbf{B}_2 \times [\mathbf{v}]) \times [\mathbf{B}]}{|(\mathbf{B}_2 \times [\mathbf{v}]) \times [\mathbf{B}]|} \tag{73}$$

$$\mathbf{n}_{MX3} = \frac{([\mathbf{B}] \times [\mathbf{v}]) \times [\mathbf{B}]}{|([\mathbf{B}] \times [\mathbf{v}]) \times [\mathbf{B}]|}, \tag{74}$$

and the velocity coplanarity,

$$\mathbf{n}_{VC} = \frac{[\mathbf{v}]}{|[\mathbf{v}]|}\,. \tag{75}$$

The solutions obtained from the RH equations in this section were calculated for two different obliquities, i.e., for perpendicular ($\theta_{B_n} = 90°$) and oblique ($\theta_{B_n} \neq 90°$) MHD shocks. In the oblique shock case, the reference frame was chosen that the magnetic field and the velocity vectors are parallel, which implies that the tangential electric field along the shock is null [15]. These solutions were used to calculate downstream from upstream plasma parameters for two different interplanetary shocks, a perpendicular shock and an oblique shock in the shock frame of reference [38]. Equation (62) is used to translate all plasma parameters from the shock reference frame to the Earth's (or spacecraft's) frame of reference.

Equations (71–75) were used to build an IP shock data base with calculated shock normals to conduct a statistical study of geomagnetic activity triggered by IP shocks with different orientations. More details about this shock study will be subjected of a forthcoming review and can be found in the literature [37–41].

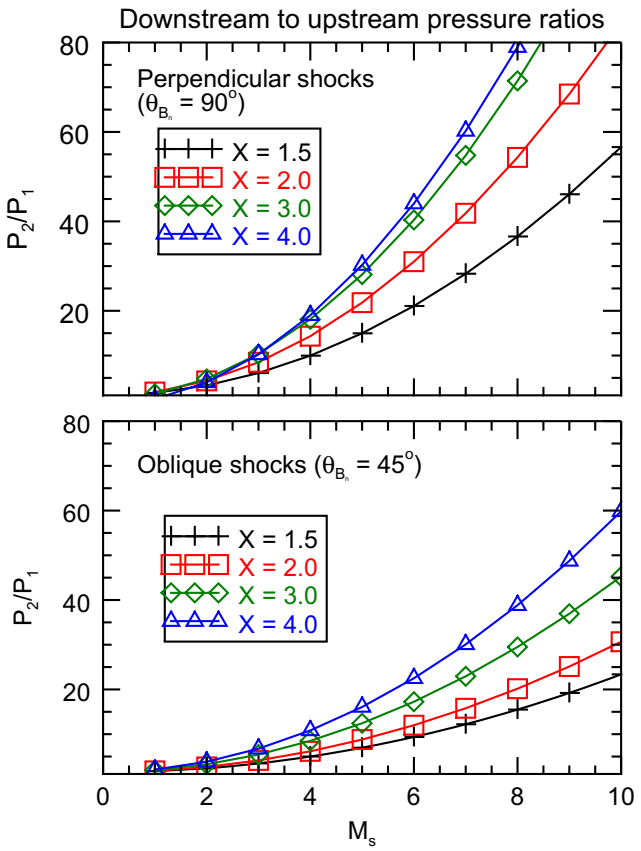

Fig. 9 Rankine-Hugoniot solutions for two types of interplanetary shocks according to their obliquities θ_{B_n}: *upper panel*, perpendicular shocks; *lower panel*, oblique shocks

4 Conclusion

In this paper, we briefly presented a review of MHD shocks in the interplanetary space at 1 AU. The main points discussed in our review are as follows:

- The derivation of the MHD equations from the Vlasov and Maxwell equations for the one- and multi-fluid MHD theories.
- From a suitable set of MHD equations, we derived the Rankine-Hugoniot equations to study how plasma parameters change through an MHD discontinuity. We then paid particular attention to a special case of MHD discontinuities, namely MHD shocks. In MHD shocks, all plasma parameters are allowed to vary through the shock surface.
- We reviewed some properties of MHD shocks with emphasis on fast forward interplanetary shocks. Sources and properties of IP shocks which in turn depend upon the angle between the upstream magnetic field vector and the shock normal vector were presented. The main sources of IP shocks observed at 1 AU are coronal mass ejections (CMEs) and corotating interaction regions (CIRs).
- The Rankine-Hugoniot solutions were solved for both the cases of perpendicular and oblique shocks. Due to the symmetry of the shock structure in the upstream region, theory suggests that the stronger and more perpendicular the shock, the higher the compression of the downstream region. This effect may lead to higher IP shock geoeffectiveness of IP shocks if the shock obliquity angle is close to 90°.

In summary, this work supplies the reader with an introductory basis on the physics of MHD shocks. The reader may find more information about IP shocks, as well as geomagnetic activity followed by IP shocks and other MHD discontinuities, in the reference list [46, 61, 64]. Finally, I would like to emphasize the importance of the shock geometry in determining the geomagnetic activity followed by IP shock interactions with the Earth's magnetosphere. Such effects have already been discussed in the literature, both with modeling [19, 38, 40, 53, 54, 66] and experimental data [26, 37, 39, 41, 63, 67]. This will be subjected for another review.

Acknowledgments This work was supported by grant AGS-1143895 from the National Science Foundation, grant FA-9550-120264 from the Air Force Office of Sponsored Research, and grants NNX13AK31G and NNG11PL02A from the National Aeronautics and Space Administration (NASA). I thank the Wind and ACE teams for the solar wind data and CDAWeb interface for data availability. I also thank the SOHO/LASCO team for the coronagraph image used in this review. The LASCO data can be downloaded from the website http://lasco-www.nrl.navy.mil. Finally, I would like to thank an anonymous reviewer for carefully evaluating this paper.

References

1. B. Abraham-Shrauner, S.H. Yun, Interplanetary shocks seen by Ames Plasma Probe on Pioneer 6 and 7. J. Geophys. Res **81**(13) (1976). doi:10.1029/JA081i013p02097
2. T. Araki, A. Shinbori, Relationship between solar wind dynamic pressure and amplitude of geomagnetic sudden commencement (SC). Earth, Planets Space **68**(9), 1–7 (2016). doi:10.1186/s40623-016-0444-y
3. A. Balogh, R.A. Treumann, *Physics of Collisionless Shocks* (Springer, New York, 2013)
4. W. Baumjohann, R.A. Treumann, *Basic Space Plasma Physics* (Imperial College Press, London, 2009)
5. D.B. Berdichevsky, A. Szabo, R.P. Lepping, A.F. Viñas, F. Mariani, Interplanetary fast shocks and associated drivers observed through the 23rd solar minimum by Wind over its first 2.5 years. J. Geophys. Res. **105**(A12), 27289–27314 (2000). doi:10.1029/1999JA000367
6. J.E. Borovsky, M.H. Denton, Differences between CME-driven storms and CIR-driven storms. J. Geophys. Res. **111**(A7) (2006). doi:10.1029/2005JA011447
7. D. Burguess, Collisionless Shocks. in *Introduction to Space Plasma Physics*, ed. by M.G. Kivelson, C.T. Russell. Chapter 5 (Cambridge University Press, Cambridge, 1995)
8. L.F. Burlaga, Hydromagnetic waves and discontinuities in the solar wind. Space Sci. Rev. **12**(5), 600–657 (1971). doi:10.1007/BF00173345
9. L.F. Burlaga, *Interplanetary Magnetohydrodynamics* (Oxford University Press, New York, 1995)
10. L.F. Burlaga, J.K. Chao, Reverse and forward slow shocks in the solar wind. J. Geophys. Res. **76**(31), 7516–7521 (1971). doi:10.1029/JA076i031p07516
11. J.K. Chao, R.P. Lepping, A correlative study of SSC's, interplanetary shocks, and solar activity. J. Geophys. Res. **79**(13), 1799–1807 (1974). doi:10.1029/JA079i013p01799
12. J.K. Chao, S. Olbert, Observation of slow shocks in interplanetary space. J. Geophys. Res. **75**(31), 6394–6397 (1970). doi:10.1029/JA075i031p06394
13. J.K. Chao, K.C. Hsieh, On determining magnetohydrodynamic shock parameters θ_{B_n} and M_A. Planet. Space Sci. **32**(5), 641–646 (1984). doi:10.1016/0032-0633(84)90115-6
14. D.S. Colburn, C.P. Sonett, Discontinuities in the solar wind. Space Sci. Rev. **439**(A11), 506 (1966). doi:10.1007/BF00240575
15. F. de Hoffmann, E. Teller, Magneto-hydrodynamic shocks. Phys. Rev. **80**(4) (1950). doi:10.1103/PhysRev.80.692
16. E. Echer, W.D. Gonzalez, L.E.A. Vieira, A.D.L.F.L. Guarnieri, A. Prestes, A.L.C. Gonzalez, N.J. Schuch, Maximum, interplanetary shock parameters during solar activity (2000) and minimum (1995-1996). Braz. Jour. Phys. **33**(1), 2301 (2003). doi:10.1590/S0103-97332003000100010
17. J.P. Edmiston, C.F. Kennel, A parametric survey of the first critical Mach number for a fast MHD shock. J. Plasma Phys. **32**(3), 429–441 (1984). doi:10.1017/S002237780000218X
18. J.T. Gosling, Coronal Mass Ejections: An Overview. in *Coronal Mass Ejections*, ed. by N. Crooker, J.A. Jocelyn, J. Feynman (American Geophysical Union, Washington, DC, 1997), pp. 9–16, doi:10.1029/GM099p0009
19. X.-C. Guo, Y.-Q. Hu, C. Wang, Earth's magnetosphere impinged by interplanetary shocks of different orientations. Chinese Phys. Lett. **22**(12), 3221–3224 (2005). doi:10.1088/0256-307X/22/12/067
20. D.A. Gurnett, A. Bhattacharjee, *Introduction to Plasma Physics With Space and Laboratory Applications* (Cambridge University Press, Cambridge University Press, 2005)

21. W.-C. Hsieh, J.-H. Shue, J.-K. Chao, T.-C. Tsai, Z. Němeček, J. Šafránková, Possible observational evidence of contact discontinuities. Geophys. Res. Lett. **41**(22) (2014). doi:10.1002/2014GL062342
22. K.G. Ivanov, Rotational discontinuities in the solar wind. Geomagn. Aeron. **11**(5), 767–770 (1971)
23. J.D. Jackson, *Classical Electrodynamics*, 3rd edn. (Wiley, Hoboken, 1999)
24. L. Jian, C.T. Russell, J.G. Luhmann, R.M. Skoug, Properties of interplanetary coronal mass ejections at one AU during 1995-2004. Solar Phys. **239**(1–2), 393–436 (2006a). doi:10.1007/s11207-006-0133-2
25. L. Jian, C.T. Russell, J.G. Luhmann, R.M. Skoug, Properties of stream interactions at one AU during 1995-2004. Solar Phys. **239**(1–2), 337–392 (2006b). doi:10.1007/s11207-006-0132-3
26. S. Jurac, J.C. Kasper, J.D. Richardson, A.J. Lazarus, Geomagnetic disturbances and their relationship to interplanetary shock parameters. Geophys. Lett. **29**(10) (2002). doi:10.1029/2001GL014034
27. C.F. Kennel, Critical Mach numbers in classical magnetohydrodynamics. J. Geophys. Res. **92**(A12), 13427–13437 (1987). doi:10.1029/JA092iA12p13427
28. C.F. Kennel, J.P. Edmiston, T. Hada, A quarter Century of Collisionless Shock Research. in *Collisionless Shocks in the Heliosphere: A Tutorial Review*, ed. by R.G. Stone, B. Tsurutani (American Geophysical Union, Washington, D.C., 1985), pp. 1–36, doi:10.1029/GM034p0001
29. M.G. Kivelson, F. Bagenal, Planetary Magnetospheres. in *Encyclopedia of the Solar System*, ed. by T. Spohn, T. Johnson, D. Breuer (Elsevier, Amsterdam, 2014)
30. L.D. Landau, E.M. Lifshitz, *Electrodynamics of Continuous Media, Course of Theoretical Physics, Volume 8* (Elsevier, Burlington, MA, 1982)
31. M.A. Lee, Coupled hydromagnetic wave excitation and ion acceleration at interplanetary traveling shocks. J. Geophys. Res. **88**(A8), 6109–6119 (1983). doi:10.1029/JA088iA08p06109
32. R.P. Lepping, P.D. Argentiero, Single spacecraft method of estimating shock normals. J. Geophys. Res. **76**(19), 4349–4359 (1971). doi:10.1029/JA076i019p04349
33. M.M. Leroy, C.C. Goodrich, D. Winske, C.S. Wu, K. Papadopoulos, Simulation of a perpendicular bow shock. Geophys. Res. Lett. **8**(12), 1269–1272 (1981). doi:10.1029/GL008i012p01269
34. I.V. Lindell, *Methods for Electromagnetic Field Analysis* (Wiley–Blackwell, Hoboken, 1996)
35. W.A. Livesey, C.F. Kennel, C.T. Russell, ISEE-1 and -2 observations of magnetic field strength overshoots in quasi-perpendicular bow shocks. Geophys. Res. Lett. **9**(9), 1037–1040 (1982). doi:10.1029/GL009i009p01037
36. J.G. Luhmann, T.-L. Zhang, S.M. Petrinec, C.T. Russell, P. Gazis, A. Barnes, Solar cycle 21 effects on the interplanetary magnetic field and related parameters at 0.7 and 1.0 AU. J. Geophys. Res. **98**(A4), 5559–5572 (1993). doi:10.1029/92JA02235
37. D.M. Oliveira, *A study of interplanetary shock geoeffectiveness controlled by impact angles using simulations and observations* (University of New Hampshire, PhD thesis, 2015)
38. D.M. Oliveira, J. Raeder, Impact angle control of interplanetary shock geoeffectiveness. J. Geophys. Res. **119**(10), 8188–8201 (2014). doi:10.1002/2014JA020275
39. D.M. Oliveira, J. Raeder, Impact angle control of interplanetary shock geoeffectiveness: a statistical study. J. Geophys. Res. **120**(6), 4313–4323 (2015). doi:10.1002/2015JA021147
40. D.M. Oliveira, M.V.D. Silveira, Space weather and interplanetary shocks. Revista Brasileira de Ensino de Física **38**(1), 1–18 (2016). doi:10.1590/S1806-11173812083
41. D.M. Oliveira, J. Raeder, B.T. Tsurutani, J.W. Gjerloev, Effects of interplanetary shock inclinations on nightside auroral power intensity. Braz. Jour. Phys. **46**(1), 97–104 (2016a). doi:10.1007/s13538-015-0389-9
42. D.M. Oliveira, E. Zesta, P.W. Schuck, E.K. Sutton, Y. Shi, On the thermosphere global time response to geomagnetic storms. J. Geophys. Res. Submitted (2016b)
43. V.J. Pizzo, The evolution of corotating stream fronts near the ecliptic plane in the inner solar system: 2. Three-dimensional tilted-dipole fronts. J. Geophys. Res. **96**(A4), 5405–5420 (1991). doi:10.1029/91JA00155
44. E.F. Priest, *Solar Magnetohydrodynamics* (D. Reidel Publishing, Dordrecht, 1981)
45. F. Reif, *Fundamentals of Statistical and Thermal Physics* (Waveland Press, Inc., Illinois, 2009)
46. A.K. Richter, K.C. Hsieh, A.H. Luttrell, E. Marsch, R. Schwenn, Review of Interplanetary Shock Phenomena Near and Within 1 AU. in *Collisionless Shocks in the Heliosphere: Reviews of Current Research*, ed. by B.T. Tsurutani, R.G. Stone (American Geophysical Union, Washington, D.C., 1985), pp. 33–50, doi:10.1029/GM035p0033
47. C.T. Russell, Overshoots in planetary bow shocks. Nature **296**(5852) (1982). doi:10.1038/296045a0
48. C.T. Russell, Planetary Bow Shocks. in *Collisionless Shocks in the Heliosphere: Reviews of Current Research*, ed. by B.T. Tsurutani, R.G. Stone (American Geophysical Union, Washington, D.C., 1985), doi:10.1029/GM035p0109
49. C.T. Russell, An Introduction to the Physics of Collisionless Shocks. in *4th Annual IGPP International Astrophysics Conference on the Physics of Collisionless Shocks*, ed. by G. Li, G.P. Zank, C.T. Russell. AIP Conference Proceedings (Am. Inst. of Phys., Washington, D.C., 2005), pp. 3–16, doi:10.1063/1.2032667
50. C.T. Russell, M. Ginskey, S.M. Petrinec, G. Le, The effect of solar wind dynamic pressure on low and mid latitude magnetic records. Geophys. Res. Lett. **19**(12), 1227–1230 (1992). doi:10.1029/92GL01161
51. C.T. Russell, Y.L. Wang, J. Raeder, R.L. Tokar, C.W. Smith, K.W. Ogivie, A.J. Lazarus, R.P. Lepping, A. Szabo, H. Kawano, T. Mukai, S. Savin, Y.L. Yermolaev, X. Zhou, B.T. Tsurutani, The interplanetary shock of September 24, 1998: arrival at Earth. J. Geophys. Res. **105**(A1), 25143–25154 (2000). doi:10.1029/2000JA900070
52. R.Z. Sagdeev, C.F. Kennel, Collisionless Shock Waves. Scientific American 40(April) (1991)
53. A.A. Samsonov, Propagation of inclined interplanetary shock through the magnetosheath. J. Atmos. Sol. Terr. Phys. **73**, 1–9 (2011). doi:10.1016/j.bbr.2011.03.031
54. A.A. Samsonov, V.A. Sergeev, M.M. Kuznetsova, D.G. Sibeck, Asymmetric magnetospheric compressions and expansions in response to impact of inclined interplanetary shock. Geophys. Res. Lett. **42**(12), 4716–4722 (2015). doi:10.1002/2015GL064294
55. S.J. Schwartz, Shock and Discontinuity Normals, Mach Numbers, and Related Parameters. in *Analysis Methods for Multi-Spacecraft Data*, ed. by G. Paschmann, I.S.R., P.W. Daly (ESA Publications Division, Netherlands, 1998)
56. Y. Shi, E. Zesta, H.K. Connor, Y.-J. Su, E.K. Sutton, C.Y. Huang, D.M. Ober, S. Delay, D.M. Oliveira, High-latitude thermosphere neutral density response to solar wind dynamic pressure enhancement. J. Geophys. Res. Submitted (2016)
57. G.L. Siscoe, J.M. Turner, A.J. Lazarus, Simultaneous plasma and magnetic-field measurements of probable tangential discontinuities in the solar wind. Solar Phys. **6**, 456–464 (1969). doi:10.1007/BF00146479

58. E.J. Smith, Identification of interplanetary tangential and rotational discontinuities. J. Geophys. Res. **78**(13), 2054–2063 (1973). doi:10.1029/JA078i013p02054
59. E.J. Smith, J.A. Slavin, R.D. Zwickl, S.J. Bame, Shocks and Storm Sudden Commencements. in *Solar Wind and Magnetosphere Coupling*, ed. by Y. Kamide, J.A. Slavin (Terra Scientific, Tokyo, 1986), p. 345
60. Z.K. Smith, M. Dryer, R.S. Steinolfson, A study of the formation, evolution, and decay of shocks in the heliosphere between 0.5 and 30.0 AU. J. Geophys. Res. **90**(A1), 217–220 (1985). doi:10.1029/JA090iA01p00217
61. R.G. Stone, B.T. Tsurutani (eds.), *Collisionless Shocks in the Heliosphere: A Tutorial Review, Geophys. Monogr. Ser.*, Vol. 34 (American Geophysical Union, Washington, D.C., 1985)
62. A. Szabo, An improved solution to the "Rankine-Hugoniot" problem. J. Geophys. Res. **99**(A8), 14737–14746 (1994). doi:10.1029/94JA00782
63. T. Takeuchi, C.T. Russell, T. Araki, Effect of the orientation of interplanetary shock on the geomagnetic sudden commencement. J. Geophys. Res. **107**(A12), 1423 (2002). doi:10.1029/2002JA009597
64. B.T. Tsurutani, G.S. Lakhina, O.P. Verkhoglyadova, W.D. Gonzalez, E. Echer, F.L. Guarnieri, A review of interplanetary discontinuities and their geomagnetic effects. J. Atmos. Sol. Terr. Phys. **73**(1), 5–19 (2011). doi:10.1016/j.jastp.2010.04.001
65. A.F. Viñas, J.D. Scudder, Fast and optimal solution to the "Rankine-Hugoniot" problem. J. Geophys. Res. **91**(A1), 39–58 (1986). doi:10.1029/JA091iA01p00039
66. C. Wang, Z.H. Huang, Y.Q. Hu, X.C. Guo, 3D global simulation of the interaction of interplanetary shocks with the magnetosphere. in *4th Annual IGPP International Astrophysics Conference on the Physics of Collisionless Shocks*, ed. by G. Li, G. Zank, C.T. Russell. AIP Conference Proceedings (Am. Inst. of Phys., Washington, D.C., 2005), pp. 320–324, doi:10.1063/1.2032716
67. C. Wang, C.X. Li, Z.H. Huang, J.D. Richardson, Effect of interplanetary shock strengths and orientations on storm sudden commencement rise times. Geophys. Res. Lett. **33**(L14104), 1–3 (2006). doi:10.1029/2006GL025966
68. Y.C. Whang, J. Zhou, R.P. Lepping, K.W. Ogilvie, Interplanetary slow shock observed from WIND. Geophys. Res. Lett. **23**(10), 1239–1242 (1996). doi:10.1029/96GL01358
69. C.-C. Wu, S.T. Wu, M. Dryer, Generation and evolution of interplanetary slow shocks. Ann. Geophys. **14**, 375–382 (1996). doi:10.1007/s00585-996-0375-1
70. M. Yan, L.C. Lee, Interaction of interplanetary shocks and rotational discontinuities with the Earth's bow shock. J. Geophys. Res. **101**(A3), 4835–4848 (1996). doi:10.1029/95JA02976
71. C. Yue, Q.G. Zong, H. Zhang, Y.F. Wang, C.J. Yuan, Z.Y. Pu, S.Y. Fu, A.T.Y. Lui, B. Yang, C.R. Wang, Geomagnetic activity triggered by interplanetary shocks. J. Geophys. Res. **115**(A00I05), 1–13 (2010). doi:10.1029/2010JA015356
72. X.-Y. Zhou, E.J. Smith, Supercriticality of ICME and CIR shocks. J. Geophys. Res. **120**(1) (2015). doi:10.1002/2014JA020700
73. X.-Y. Zhou, B.T. Tsurutani, Rapid intensification and propagation of the dayside aurora: large scale interplanetary pressure pulses (fast shocks). Geophys. Res. Lett. **26**(8), 1097–1100 (1999). doi:10.1029/1999GL900173
74. T.H. Zurbuchen, I.G. Richardson, In-situ solar wind and magnetic field signatures of interplanetary coronal mass ejections. Space Sci. Rev. **123**(1–3) (2006). doi:10.1007/s11214-006-9010-4